ISSN Print: 2394-7500
ISSN Online: 2394-5869
Impact Factor: 5.2
IJAR 2016; 2(5): 175-180
www.allresearchjournal.com
Received: 07-03-2016
Accepted: 08-04-2016

AS Jagadisha
Department of Physics,
Kuvempu University,
Shankarghatta, Karnataka,
India-577 451

E Nagaraja
Department of Physics,
Kuvempu University,
Shankarghatta, Karnataka,
India-577 451

NB Desai
Department of Physics,
Kuvempu University,
Shankarghatta, Karnataka,
India-577 451

HS Jayanna
Department of Physics,
Kuvempu University,
Shankarghatta, Karnataka,
India-577 451

Correspondence
HS Jayanna
Department of Physics,
Kuvempu University,
Shankarghatta, Karnataka,
India-577 451

Effect of gamma ray irradiation on structural and electrical properties of $Mg_{(1-x)}Zn_x$ Ferrite

AS Jagadisha, E Nagaraja, NB Desai, HS Jayanna

Abstract
The Mg-Zn ferrites with a composition of $Mg_{(1-x)}Zn_xFe_2O_4$ *(X= 0.2, 0.4, 0.6, and 0.8)* ferrite powders have been successfully prepared by solid state reaction. Phase purity of the samples has been confirmed by X-ray diffraction. Morphological and elemental compositions of the prepared samples were studied by high resolution scanning electron microscopy and energy dispersive spectroscopy (EDS). The prepared samples were irradiated by high energy gamma radiation of ^{60}Co source of dose rate 6.972 k Gy per hour (dose: 300 kGy and 500 kGy). The XRD spectra are obtained for the irradiated samples and compared with that of the pristine samples to study the changes in the structure. The DC electrical conductivity at room temperature was studied. The obtained result shows an increase in crystallite size and DC electrical conductivity at room temperature with increase of radiation dose and decrease in activation energies.

Keywords: gamma irradiation, Mg Zn ferrite, magnetic materials

1. Introduction
In the field of technological applications, the ferrites have gained a much importance due to their combined characteristics of magnetic conductors and electrical insulators. The polycrystalline ferrites have a wide range of applications in microwave to radiowave frequencies of electromagnetic spectrum [1]. Ferrites with spinel structure represent the important class of magnetic materials. The combination of magnetic and electrical properties makes ferrite useful in many technological applications

The electrical and magnetic properties of such ferrites depend strongly on distribution of cations at the tetrahedral (A) and octahedral (B) sites in the lattice [2, 3]. It has been identified that zinc ions may be used to modify the saturation magnetization. It was observed that the addition of zinc ions also affects the lattice parameter and it would be expected to change the Curie temperature of the material [4]. The replacement of divalent ions in pure ferrite leads to the modification of the structural, electrical and magnetic properties [5].

A special feature of these materials is that these materials are used in different range of frequencies by substituting different ions in the chemical formula unit and the control of the processing steps. Ferrites are broadly used in magnetic recording, information storage, colour imaging, bio-processing, magnetic refrigeration and in magneto optical devices [6, 7].

The irradiation of energetic radiation on the certain materials may produce the changes permanently [8]. The radiation induced change in these materials depends on absorbed energy by the material. Hence it has gained importance in the recent years due to large inventions in the field of electronic and technological industries, nuclear facilities, accelerators, space crafts, space vehicles and satellites. Gamma radiations can produce defects of various types such as point defect, cluster, and ionization of atoms. The effect of gamma radiation on several ferrites are reported, [9, 13]. The absorption of large amount of gamma radiation may alter the structural properties.

The earlier reports were says, both diffusion co efficient of oxygen ion and the lattice parameter were increased in case of Co-Zn ferrite by gamma rays [11]. And also dielectric, thermoelectric power and thermal conductivity of Co Zn ferrite [7, 23] and electrical Properties of Mg-Cu-Zn ferrites were studied [17]. The gamma irradiation improves the magnetic properties of Mg –Mn and Mn-Ni ferrite nano particles [12].

In the present study we report the synthesis, characterization and effect of gamma irradiation on Mg-Zn ferrite.

2. Experimental

In the present work, we use the conventional ceramic technique to synthesize the Mg-Zn ferrites powder. The Mg-Zn ferrites having general formula $Mg_{(1-x)}Zn_xFe_2O_4$ (where x = 0.2, 0.4, 0.6, 0.8) were prepared by solid state reaction. The AR grade Magnesium oxide, Zinc oxide, and Ferric oxide were weighed carefully on single pan microbalance (LC: 0.1mg) to have proper stoichiometric ratio required in the final product.

The composition was grounded into a very fine powder using an agate morter, and then pre-sintered at 800°C for 8 hours. The compositions were grounded again and pressed in the form of pellets, then sintered at 1200°C for 12 hours and slowly cooled to room temperature

The formation of spinel phase and crystal structure was confirmed by X-ray diffraction using Cu$K\alpha$ radiation of wavelength 1.5405 $A°$ from the X-ray diffractometer over the 2θ range of 10°-60° with a scanning rate of 2 degree per minute.

The samples were irradiated with the energetic gamma radiation with energy 6.972 kGy/h. The irradiation source is ^{60}Co gamma cell, located at Centre for Application of Radioisotopes and Radiation Technology (CARRT), Mangalore University, India.

The average crystallite size of the prepared ferrite samples were determined from the full width at half maximum (FWHM) of most intense peak (311) using Debye-Scherrer equation.

$$D = \frac{k\lambda}{\beta \cos\theta} \qquad \ldots(1)$$

Where, k is Scherrer factor (0.9), λ is the wavelength of X-ray, and is 1.5046 $A°$, β is the angular line width at half maximum intensity and θ is the Bragg angle of actual peak.

Micro structural analysis of the prepared samples was carried out by scanning Electron microscopy (SEM) and elemental compositional analysis of all samples was done by Energy Dispersive Spectroscopy (EDS).

For measuring the electrical conductivity, the samples were inserted between two silver electrodes where the silver paste was used as a contact material. The conductivity of the sample (σ) was calculated using the relation

$$\sigma = d/RA \qquad (2)$$

Where, A and d are the cross-section area and the thickness of the sample, respectively. R is the resistance of the sample.

3. Results and discussions

3.1 XRD measurement

The room temperature X-ray diffraction patterns of all the samples (x = 0.2, 0.4, 0.6, 0.8) of Mg-Zn ferrite, before and after gamma irradiation are shown in Figure. 1. X-ray diffraction pattern shows all the allowed reflection lines corresponding to cubic spinel phase and also showed slight shift in the peak position, decrease in relative intensity and increasing of crystallite size. The similar results were observed in earlier reports [9, 13, 22].

The increase in particle size is due to formation of ferrous ions (Fe^{2+}) which have large radius than that of ferric ions (Fe^{3+}) [11, 13]. Due to gamma irradiation the distorted lattice is formed, the dependence of lattice parameter on (Zn^{2+}) ecomes nonlinear [11].

It is well known that the Zn^{2+} ions occupy the tetrahedral sites (A-sites) and most of Mg^{2+} ions occupy octahedral sites (B-sites). Starting from the basic ferrite $MgFe_2O_4$, Zn^{2+} ions are substituted to replace Mg^{2+} ions. The replacement takes place by the movement of Fe^{3+} ions from A-sites to B-sites. The radius of tetrahedral site remains same before and after irradiation. Whereas radius of octahedral site is higher than before irradiation due to formation of ferrous ions [11]. The calculated average ferrite crystallite size for samples are listed in the table 1below,

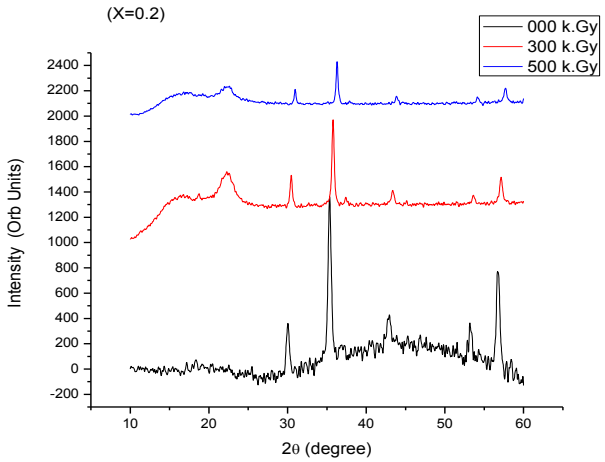

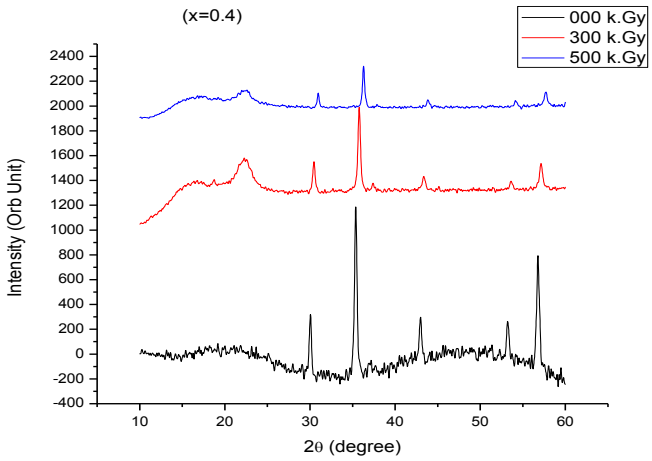

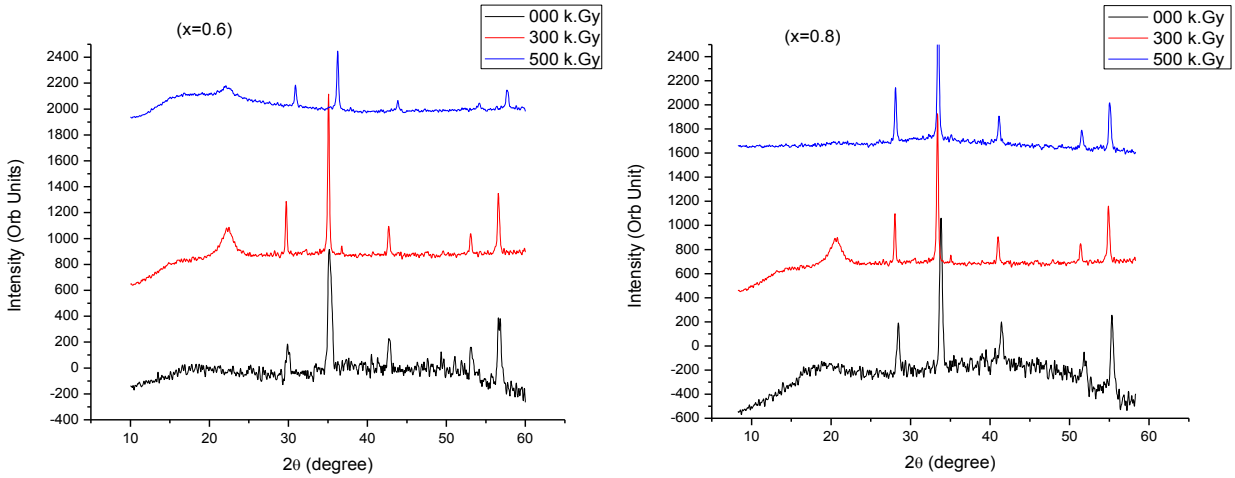

Fig 1: XRD pattern for un- irradiated and irradiated samples of Mg-Zn ferrite.

Table 1: Variation of crystallite size before and after irradiation.

Composition	Crystallite size in nm		
	Before irradiation	After irradiation	
		300 KGy	500 KGy
X=0.2	163	174	177
X=0.4	152	163	179
X=0.6	133	148	163
X=0.8	122	128	133

3.2 SEM Studies

Scanning electron microscopy analysis was performed in order to investigate the microstructure and morphology of irradiated and unirradiated ferrite samples using FEIXL 40 SIRION FEG digital scanning microscope.

X	Un irradiated sample	300 kGy	500 kGy
0.2	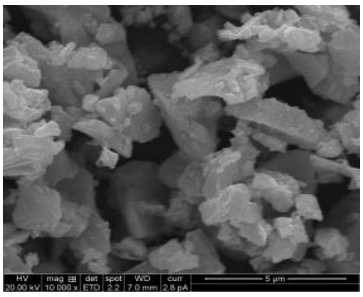	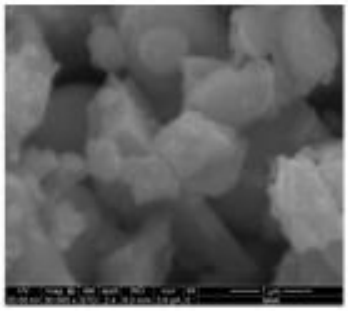	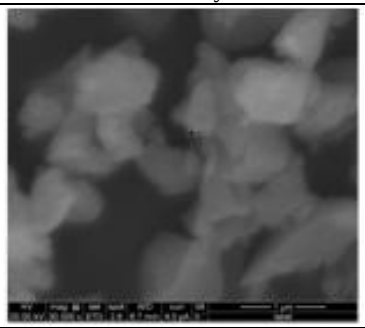
0.4	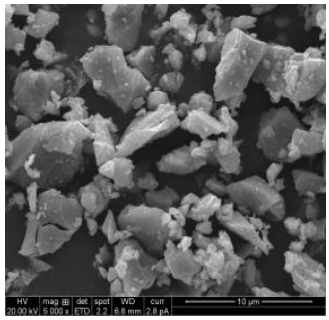	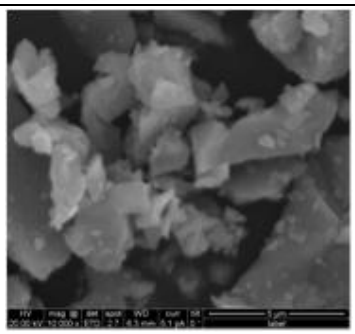	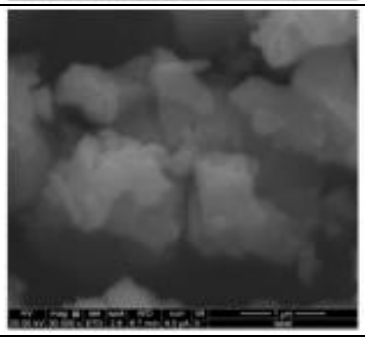
0.6	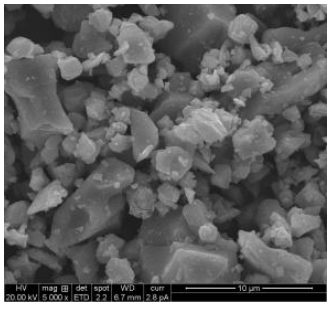	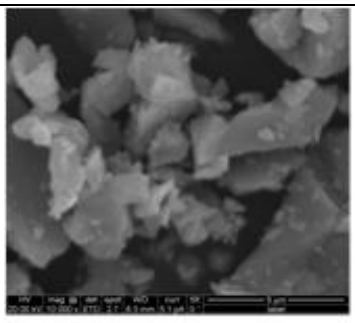	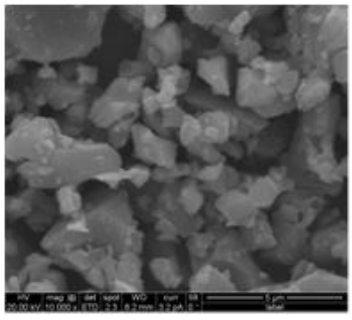

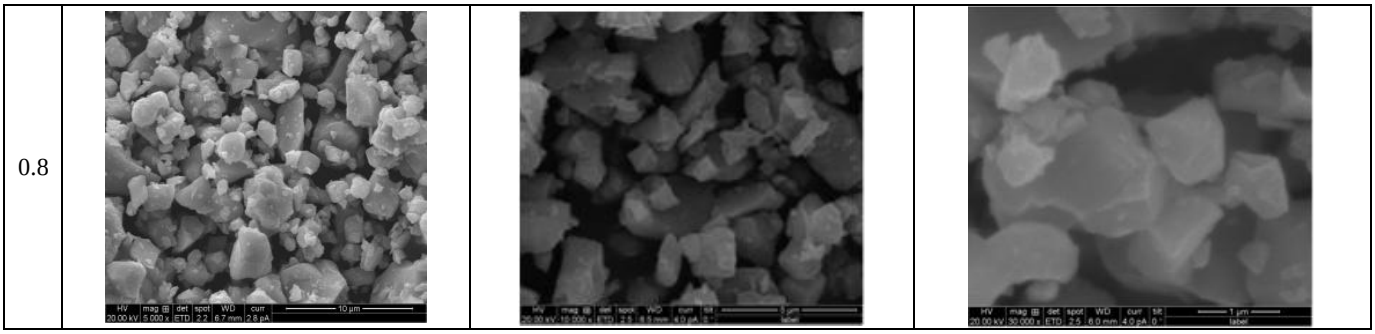

Fig 2: SEM morphology of synthesized ferrite. (Before and after irradiation)

The images show that the particles have an almost homogeneous distribution, and some of them are in agglomerated form. It is evidenced by SEM images that the particles are in nano meter range. The particles were observed as uniform grains (in different SEM images) confirming the crystalline structure of Mg-Zn ferrites which were detected by XRD studies.

3.3 Elemental Analysis by EDS

The elemental analysis of all the Mg-Zn ferrite samples with different compositions were analyzed by Energy Dispersive Spectrometer (EDS) and the elemental percentage (%) and atomic percentage (%) of different elements in the samples were shown in the Table 2. The EDS pattern of samples with x = 0.2, 0.4, 0.6, and 0.8 are shown in Figure 3 which indicates the elemental and atomic composition of the samples.

Table 2: ED's analysis of elemental percentage and atomic percentage of prepared samples

Element	X=0.2		X=0.4		X=0.6		X=0.8	
	Wt (%)	At (%)	Wt (%)	At (%)	Wt (%)	At (%)	Wt (%)	At (%)
O	8.20	24.32	8.63	24.67	8.92	24.80	9.03	24.46
Mg	1.13	2.21	3.03	5.70	4.46	8.16	6.02	10.73
Fe	61.57	52.34	65.64	53.75	70.05	55.77	75.22	58.36
Zn	29.09	21.13	22.70	15.88	16.56	11.27	9.73	6.45

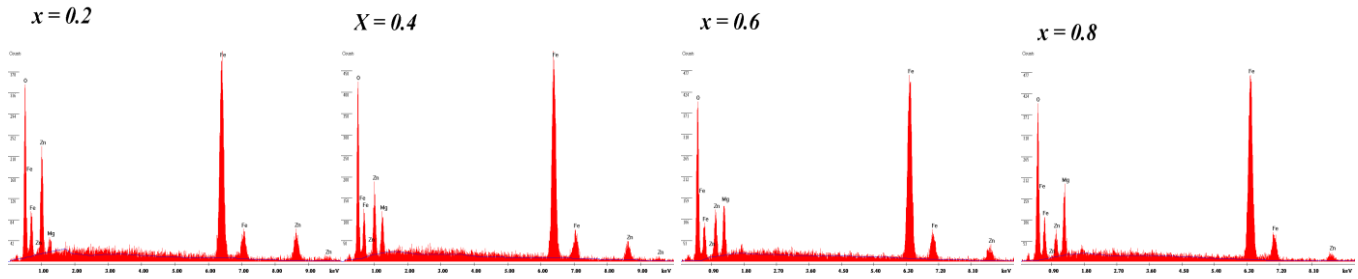

Fig 3: EDS pattern of prepared Mg Zn ferrites.

3.4 D C Electrical Conductivity at Room Temperature.

The variation of DC Conductivity at room temperature, before and after irradiation for the sample $Mg_{(1-X)}\ Zn_X\ Fe_2O_4\ (X\ =\ 0.2,\ 0.4,\ 0.6,\&\ 0.8)$ were shown in Figure 4

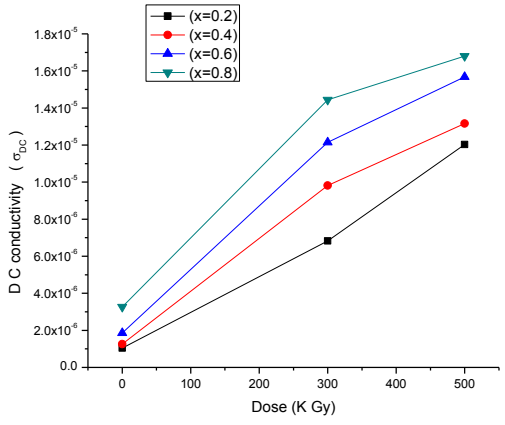

Fig 4: Variation DC conductivity with irradiation dose.

DC conductivity of the synthesized samples was increased with composition and as well as with radiation dose for all the samples.

According to previous studies, it was reported that the DC conductivity of the ferrites are influenced by the concentration of Fe^{2+} ions and porosity of the sample [16]. The decrease in concentration of ferrous ions (Fe^{2+}) confines the probability of hoping mechanism of conduction electrons between ferrous ions (Fe^{2+}) and ferric ions (Fe^{3+}) in B sites. On the other hand, increasing in the porosity obstruct the movement of charge carriers [17, 18]. In case of Mg Zn Ferrite, the B sites are occupied by both Mg^{2+} ions and Fe^{3+} ions and Zn^{2+} ions [18, 19]. The following equilibrium may exist during sintering process [17] $Fe^{3+} + Zn^{1+} \leftrightarrow Fe^{2+}+Zn^{2+}$.The ratio of ferrous ions to ferric ions on B site dominates the porosity, and similar results were reported by several researchers for several types of Ferrites [9, 21, 17, 19].

DC electrical conductivity of the irradiated samples were increased with dose. The increase in electrical conductivity can be explained with following interaction [22].

$$Mg^{2+} + \gamma \leftrightharpoons Mg^{3+} + e$$

This interaction leads to an increase in the ratio of Mg^{2+}/Mg^{3+} lying in the octahedral sites and in turn increase the hoping rate after irradiation, consequently increase in electrical conductivity.

3.5 Temperature dependence of D C Electrical Conductivity.

The Figure 5 shows the temperature dependence of the DC conductivity, before and after irradiation, for $Mg_{(1-X)}\ Zn_X\ Fe_2O_4\ (X = 0.2,\ 0.4,\ 0.6, \& 0.8)$

The activation energy are calculated in the paramagnetic region, E_p and in the ferromagnetic region, E_f .and are found to increase with irradiation in all the samples.

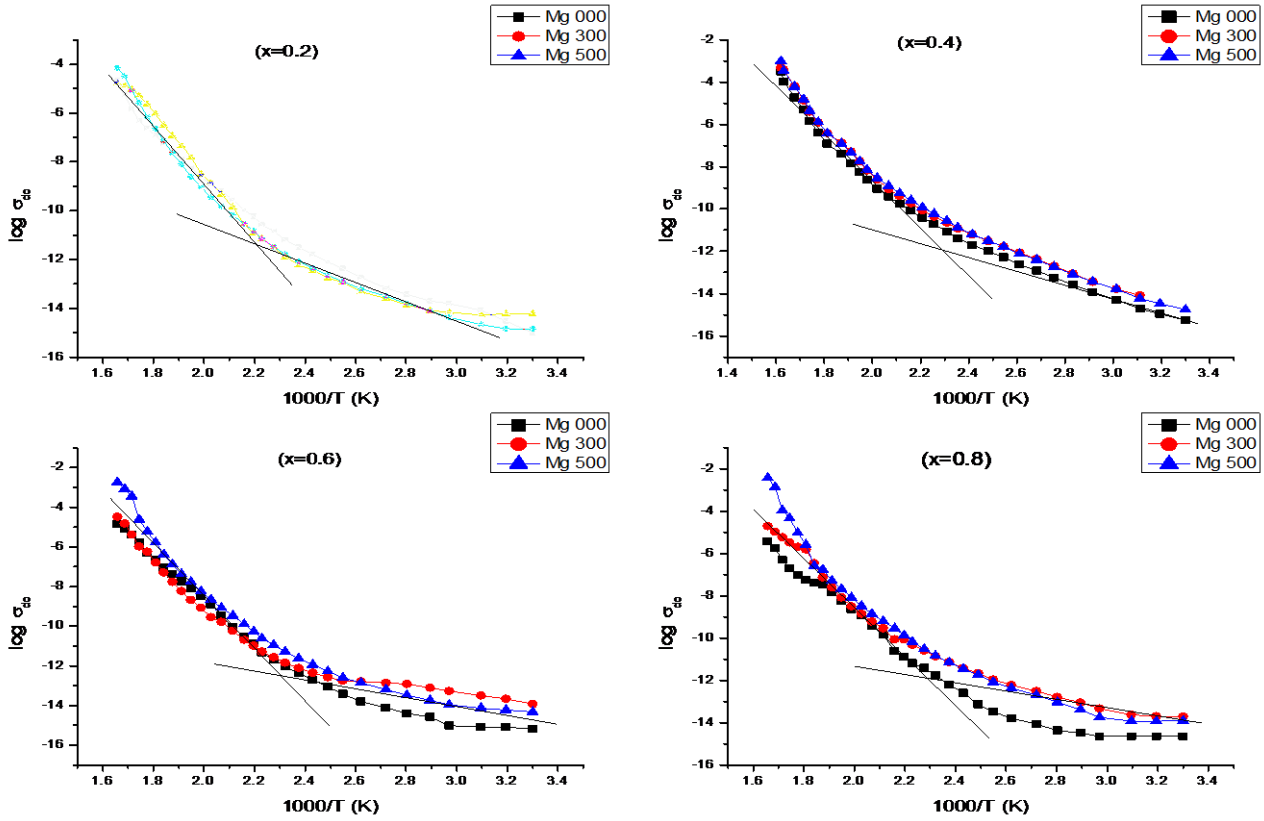

Fig 5: Temperature dependent DC electrical conductivity of $Mg_{(1-X)}\ Zn_X\ Fe_2O_4\ (X = 0.2\ \ 0.4, 0.6, \& 0.8)$

From Figure 5, it was observed that the electrical conductivity decreases with temperature for all samples. This response resembles the semiconductor nature and it could be explained by Arrhenius relation [19, 20].

$$\sigma = A \exp(-\Delta E/kT) \qquad \ldots (3)$$

Where, A is a temperature independent constant, k is the Boltzman constant $(8.617 \times 10^{-5}\ eV\ K^{-1})$, ΔE is the activation energy and T is the absolute temperature. It is observed that the activation energy decreased after irradiation in both the region.

The decrease in activation energy may be due to generation of some vacancies at different depth, which acts as trapping centers causes depressing of the jumping length of electron

4. Conclusions

X ray diffraction patterns of all the samples show single phase cubic spinel structure and contain all major peaks, before and after irradiation. The peak shift and decrease in intensity were observed. These results indicate formation of ferric centers and induced defects.

The DC electrical conductivity of the irradiated samples was found to be increased with dose. This is due to increase in the ratio of Fe^{2+}/Fe^{3+} in octahedral sites by hoping mechanism. The activation energy of the samples was decreased with dose, due to generation of vacancies.

5. Acknowledgements

The authors wish to thank the Centre for Application of Radioisotopes and Radiation Technology (CARRT), Mangalore University, India and Dr H M Somashekarappa (Head, CARRT).

6. References

1. Smit J, Verweel J. Ferrites at radio frequencies, McGraw-Hill, New York, 1971.
2. Dormann JL, Nogues M. J Phy Cond Mat. 1990; 2(5).
3. Rezlescu N, Rezlescu E, Pasnicu C, Craus ML. *J Phy Cond Mat.* 1994; 6(29):5707-5716.
4. El-Sayed AM. Ceramics International 2002; 28(4):363-367.
5. Zhong Z, Li Q, Zhang YL, Zhong HS, Cheng M, Zhang Y. Powder Technology, 2005; 155(3):193-195.
6. Hirai T, Kobayashi J, Koasawa I. Langmuir, 1999; 15(19):6291-6298.
7. Kodama RH. Journal of Magnetism and Magnetic Materials. 1999; 200(1):359-372.
8. Hemeda OM. Phase Transition 1994; 51:87.
9. Ateia E, Egypt J. Solids, 2006; 29:317-328.
10. Tashtoush NM. Am. J. Applied Sci. 2005; 2:887-891.

11. Hemeda OM, El-Saadawy M. J Magn Mater. 2003; 256:63-68.
12. Okasha N. J Alloys Compd. 2010; 490:307-310.
13. Hassan HE, Sharshar T, Hssien MM. Hemeda OM. Nucl. Instr. Meth. B 2013; 304:72-79.
14. ahamed MA, El-dek SI, Masour N. Omksha, solid state Sci 2011; 13:1180-1186.
15. Prashanth KS, Rao Sheeja Krishnan, Manjunath Patttabi, Ganesh Sanjeev, Int. J Chem Tech Res. 2015; 7(3):1377-1380.
16. Sattar AA, El-Sayed HM, Eltabey MM. J Mater Sci. 2005; 40:4873-4873.
17. Mohamed Eltabey H, Ebrahim Hassan, Ismail Abd, Elrahim Ali. Am. J App Sci 2014; 11(1):109-118.
18. Murthy SR. Bull. Mater. Sci., 2001; 24:379-383. DOI: 10.1007/BF02708634
19. Yue Z, Zhou J, Li L, Wang X, Gui Z. Mater. Sci. Eng., B, 2001; 86:64-69.
20. Shinde AB. IJITEE 2013; 3(4):64-67.
21. Ahmed MA, El-dek SI, Mansour SF, Okasha N. Solid State Sci. 2011; 13:1180-1186.
22. El-Tabey MM, Ali IA, Hassan HE, MNH Sosan. J Matter. Sci. 2011; 46:2294-2299.
23. Tawfik A, Hamada IM, Hemeda OM, Mag. mater JM. 2002; 250:77-82.